에너지공학, 제26권 제1호(2017)
Journal of Energy Engineering, Vol. 26, No. 1, pp.9~22(2017)
https://doi.org/10.5855/ENERGY.2017.26.1.009

Thermal-flow analysis of a simple LTD (Low-Temperature-Differential) heat engine

Kim Yeongmin · Kim Won Sik · Jung Haejun · Chen Kuan* · Chun Wongee †
Department of Nuclear and Energy Engineering, Jeju National University, Jeju 63243, Korea
*Department of Mechanical Engineering, University of Utah, Salt Lake City, Utah 84112, U.S.A.
(Received 1 February 2017, Revised 16 February 2017, Accepted 27 February 2017)

Abstract

A combined thermal and flow analysis was carried out to study the behavior and performance of a small, commercial LTD (Low-Temperature-Differential) heat engine. Laminar-flow solutions for annulus and channel flows were employed to estimate the viscous drags on the piston and the displacer and the pressure difference across the displacer. Temperature correction factors were introduced to account for the departure from the ideal heat transfer processes. The analysis results indicate that the work required to overcome the viscous drags on engine moving parts and to move the displacer is much smaller than the moving-boundary work produced by the power piston for temperature differentials in the neighborhood of 20℃ and engine speeds below 10 RPS. A comparison with experimental data reveals large degradations from the ideal heat transfer processes. Thus, heat-transfer devices inside the displacer cylinder are recommended.

Key words : Low-temperature-differential engine, Stirling cycle, Thermal-flow analysis, Waste heat.

1. Introduction

Waste heat at temperatures a couple of dozen degrees above the ambient temperature is a vast energy source. This low-grade thermal energy is mainly discharged from power plants and A/C systems. Because the conversion efficiencies of power plants are typically only about 30 % and the amount of heat discharged from an A/C system is equal to the heat removed from the cooled space plus the heat converted from work input, a tremendous amount of very low-temperature waste heat is produced daily from power plants, A/C systems, as well as other industrial plants and processes around the world. This abundant energy source has being used directly for space heating or as the heat source in heat pumping - applications, but has seldom been utilized for (mechanical or electrical) power generation.

According to the Carnot principles [1], the maximum thermal efficiency for a heat engine operating between thermal energy reservoirs at 20 and 50℃ is only 9%. In addition, a 5 to 10℃ temperature difference is often required for effective heat transfer between the heat engine and its surroundings. The low conversion efficiency (due to low temperature differential) and power output (due to low heat transfer rates) have led to little interest in LTD (Low-Temperature-Differential) engine researches and the slow development of this kind of energy converters in the past. The recent concerns about sustainability and environmental awareness have attracted increased interest and attention on wider and more efficient use of low-temperature waste heat, in particular the heat discharged from large power plants and A/C systems. If this free energy could be

†To whom corresponding should be addressed.
Tel : +82-64-754-3646 E-mail : wgchun@jejunu.ac.kr

used to generate power, the emissions of greenhouse gases and thermal pollutions to the environment would be greatly reduced. The fuel or electricity costs of power plants or A/C systems would drop, too.

Of the various thermal-to-mechanical or -electrical energy conversion techniques, TE (thermoelectric) generators and SMA (shape-memory alloy) heat engines have been proven to be feasible for temperature differentials of only a few dozen degrees Celsius. SMA engines had received a lot of attention a few decades ago, and a variety of SMA materials and engine designs have been explored to improve the conversion efficiency and power output [2]. The simplest SMA engine consisted of a SMA wire wrapped around 2 pulleys, with one pulley dipped in a hot water bath and the other cooled by the ambient air. Because the working substances of SMA engines are in the solid phase and solids have higher thermal inertia (per unit volume) than gases, the changes in substance temperatures and shapes are slower. Heat sources with temperatures 50℃ above the ambient temperature or higher and slender-structural SMA materials are often needed for fast shape changes.

The TE generator is probably the most popular choice by far for direct thermal-to- electric energy conversion at very low temperature differentials. TE devices have been developed to generate a small amount of electricity from body heat which was only a couple of dozen degrees above the ambient temperature. The generated electricity was used to power watches, handheld flashlights, or other small electronic devices. The hot and cold ends of a TE device is typically only a few millimeters apart, and TE materials have high thermal conductivities. As a result, heat transfer in a TE generator is much more effective than heat transfer in a heat engine that utilizes a gas as the working fluid. The high heat transfer rate in a TE generator translates into high power output, but its conversion efficiency is low due to heat leakage between the closely separated hot and cold ends of this type of energy converters [3]. If conversion efficiency is more important than power output, heat engines that operate on the Stirling cycle or its variations are more promising to approach the maximum possible efficiency predicated by the second law of Thermodynamics [1]. Also theoretically, the conversion efficiency from mechanical energy to electricity can be 100% [4].

The Stirling cycle has the same efficiency as the Carnot cycle operating between the same temperature limits. Unlike the Carnot heat engine, are generator is required in the Stirling engine to store the heat removed from the working fluid during the constant-volume heat removal process. The stored thermal energy is later released to pre-heat the working fluid before heat input from an external heat source takes place. A complicated mechanism is also needed to keep the volume of the working fluid constant when flowing through the regenerator.

The first engine operating on the Stirling cycle was invented and patented by Robert Stirling in 1816 [5]. Based upon Stirling's original design, the Stirling engine had evolved into many different forms and sizes in the nineteenth century. It had been a popular heat engine because of its simple design and easy and safe operation [6]. Being an external-combustion device, the Stirling engine had a low noise level. The small Stirling engines developed in the nineteenth century were capable of producing mechanical power ranging from 100 to 4000W. The rapid developments of internal-combustion engines and electric motors in late nineteenth century and early twentieth century ended the first era of the Stirling engine.

At present, many LTD heat engines capable of utilizing low- grade thermal energy are commercially available. These engines can run on temperature differentials ranging from 90 down to a few degrees Celsius. Alveno et al. [7] tested 3 commercial LTD engines of similar design, and found the one with concentric power and displacer cylinders (This engine configuration is similar to the Beta-type Stirling engine) could run on the smallest temperature difference, but the American Stirling Company MM-7 en-

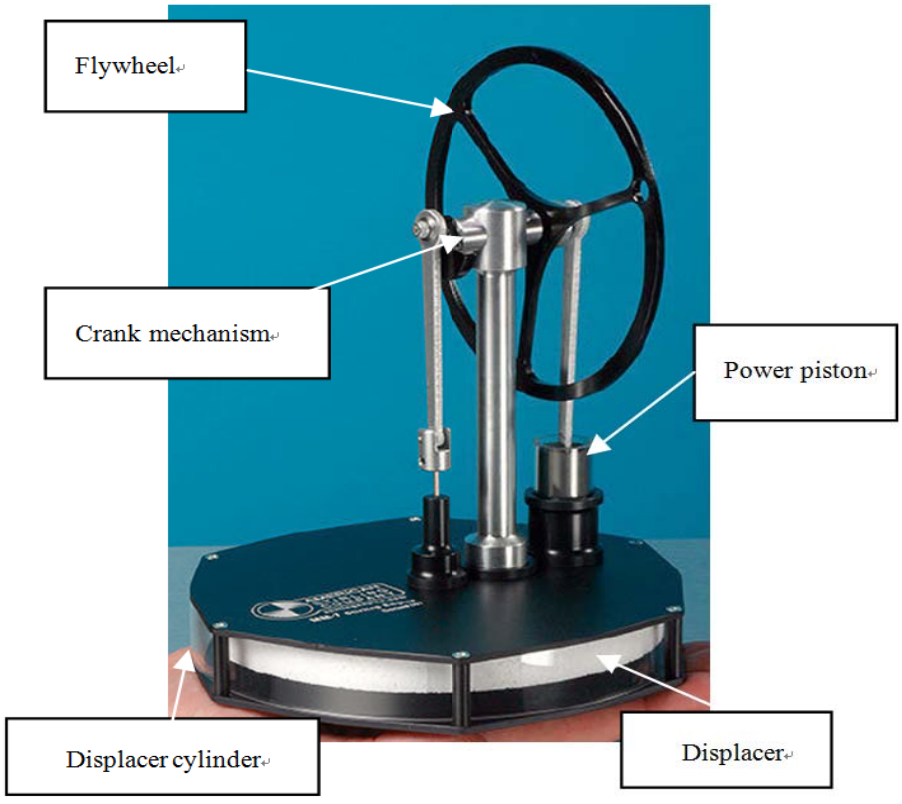

Fig. 1. The American Stirling Company MM-7 engine.

gine, which had the largest heat transfer surface area, produced the highest power output. The MM-7 engine, which is similar to the Gamma-type Stirling engine, was selected in the present theoretical investigation of LTD engines. This engine was also selected by Aragon-Gonzalez et al. in their experimental study of low-cost LTD engines [8].

As can be seen in Fig. 1, the MM-7 engine uses a very simple crank mechanism to reduce the cost and the construction and operation complexities. It also lacks of an effective regenerator for internal heat exchange between the working fluids at high and low pressures. These changes in engine design have made the MM-7 engine different from the "true" Stirling engine in 2 major ways. First, the regeneration process of the MM-7 engine does not take place at constant volume. The second departure from the true Stirling engine cycle is that the working fluid is not at the heat source or sink temperature when entering the hot or cold end of the displacer cylinder. The conversion efficiencies of the MM-7 engine and other LTD engines of similar design therefore are lower than that of the Carnot or Stirling engine even under the ideal operating conditions in which all frictional losses are eliminated and all heat transfer processes occur across an infinitesimally small temperature difference.

Simplified thermodynamic analyses of the Stirling engine can be found in Senft's book [6]. Presented in this paper is a combined thermal-flow analysis of the MM-7 engine in which the frictional losses of the working fluid were calculated for different engine speeds and temperature differentials. Temperature correction factors were introduced to take into account the departure from the ideal heat transfer processes. The powers required to overcome the viscous friction of the working fluid and the pressure difference across the displacer were found to be much smaller than the power produced by the power piston for engine speeds below 10 RPS (revolutions

per second). Compared with the power outputs measured in experiments [7, 8], the difference between the working fluid temperature and the heat source or sink temperature during heat addition or rejection was very large for the MM-7 engine at speeds higher than 1 RPS. The mathematical model and analytical solution developed in the present investigation for the MM-7 engine can be easily modified and applied to other LTD heat engines of similar design.

2. Thermal – flow analysis of the MM–7 engine

A simple cranking mechanism is employed in the MM-7 engine to convert the linear movements of the power piston and the displacer to rotational movements. The linear movements are both sinusoidal and have the same frequency, but the strokes are different, and there is a phase lag between the piston and displacer movements. Referring to the drawing in Fig. 2, the relationships between the linear movements of the piston and the displacer and the angular displacement of the engine shaft are:

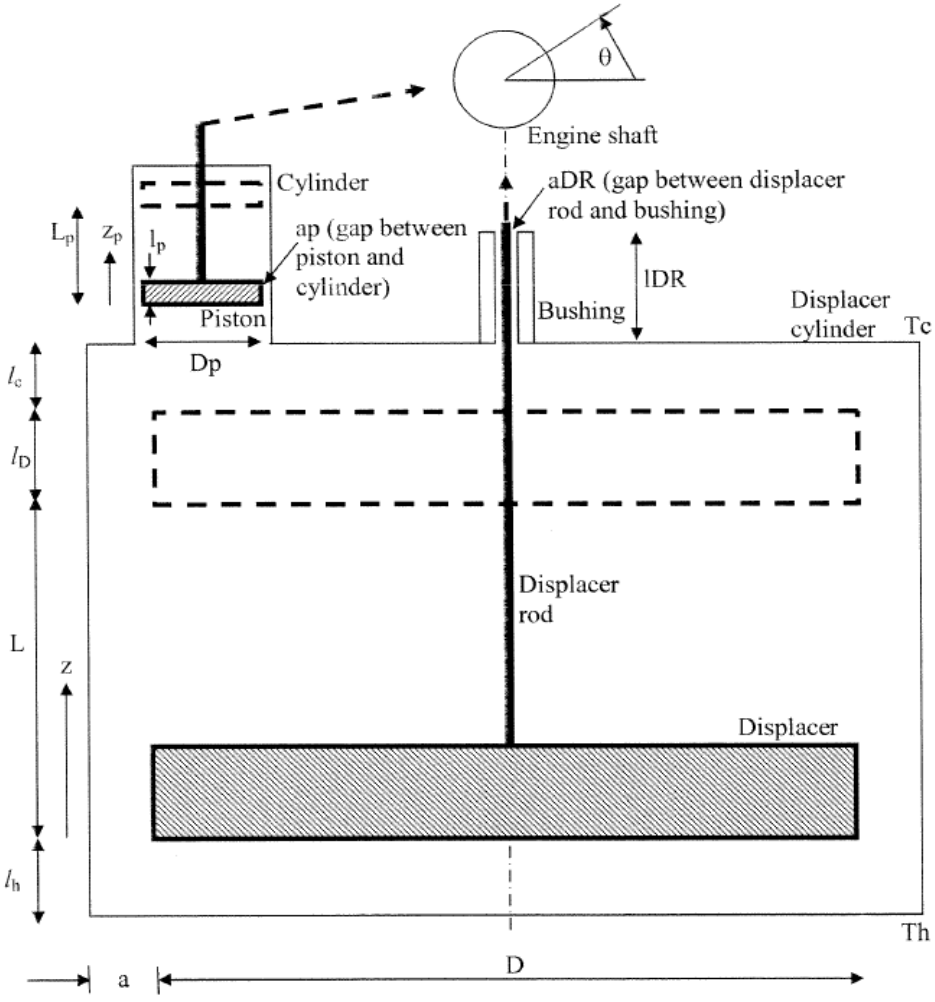

Fig. 2. Nomenclature and major components of the MM-7 engine.

$$z = \frac{L}{2}[1 + \cos(\theta)] \quad (1)$$

$$zp = \frac{Lp}{2}[1 + \cos(\theta + \alpha)] \quad (2)$$

where z and zp are the vertical positions of the displacer and the piston, and α is the phase difference between the movements of the piston and the displacer. The displacer is in its highest position (z = L) at Θ = 0. Plotted in Fig. 3 are the vertical positions of the piston and the displacer as functions of the crank angle for α = - 90 degrees. This is the phase angle that yields the highest theoretical engine power output. For a constant engine speed, the time variable (t, in seconds) is equal to the abscesses of the plot in Fig. 3 divided by 2π and by the engine speed (in RPS).

The vertical velocities of the displacer and the piston are the time derivatives of their positions:

$$Uz = \frac{dz}{dt} = -\frac{L}{2}\sin(\theta)\frac{d\theta}{dt} = -\frac{L}{2}\sin(\theta)\,\omega \quad (3)$$

$$Uzp = \frac{dzp}{dt} = -\frac{Lp}{2}\sin(\theta + \alpha)\frac{d\theta}{dt} \quad (4)$$

It should be pointed out that, some Stirling engines use a sophisticated crank mechanism to enhance the engine power out. The linear movements of these engines may not be sinusoidal functions of the crank angle.

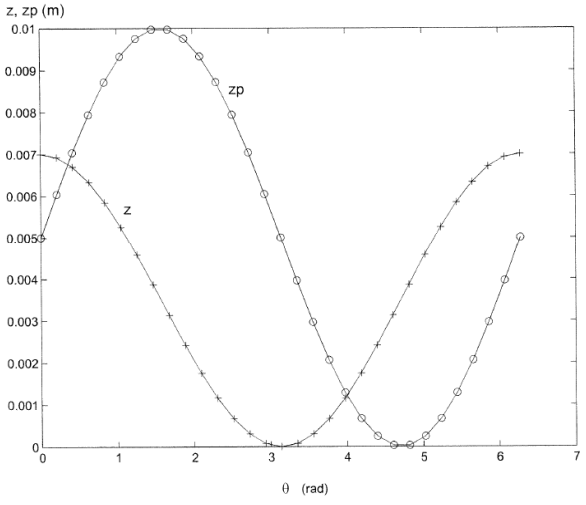

Fig. 3. Piston and displacer positions for α = - 90°.

As depicted in Fig. 4, the volume of air in the cold region of the engine is the sum of the air volume in the power cylinder (= V_p + V_{pd}) and the air volume above the displacer in the displacer cylinder (= V_{cd} + V_{cD}). The volume of air in the hot region of the engine is the volume below the displacer (= V_{hD} + V_{hd}). V_p in Fig. 4 is the volume swept by the piston. V_{pd} is the clearance of the power cylinder. V_{cd} and V_{hd} are the upper and lower clearances of the displacer cylinder. V_{cD} and V_{hD} are the volumes swept by the displacer above and below the displacer. The swept volumes can be expressed as functions of the shaft angle, the piston or displacer radius, and the strokes:

$$Vp = Ap\,zp = \pi rp^2\frac{Lp}{2}[1 + \cos(\theta + \alpha)] \quad (5)$$

$$VcD = ADc\left\{L - \frac{L}{2}[1 + \cos(\theta)]\right\} \quad (6)$$

$$VhD = ADc\left[\frac{L}{2}[1 + \cos(\theta)]\right] \quad (7)$$

Because of the small size and low speeds of the MM-7 engine, it is reasonable to assume that the air flow in the engine is laminar. The rate of airflow from the cold to the hot region of the engine depends on the pressure difference across the displacer and the viscous force on the lateral surface of the displacer. The flow through the annulus of the displacer is simplified to the Couette-Poiseuille flow as a first approximation. The volume flow rate therefore can be estimated from the following equation:

$$Qv = \pi D\left(\frac{Uz\,a}{2} - \frac{1}{12\mu}\frac{dp}{dz}a^3\right) = -ADc\,Uz \quad (8)$$

Using the above equation, the pressure gradient in the displacer annulus can be related to the engine

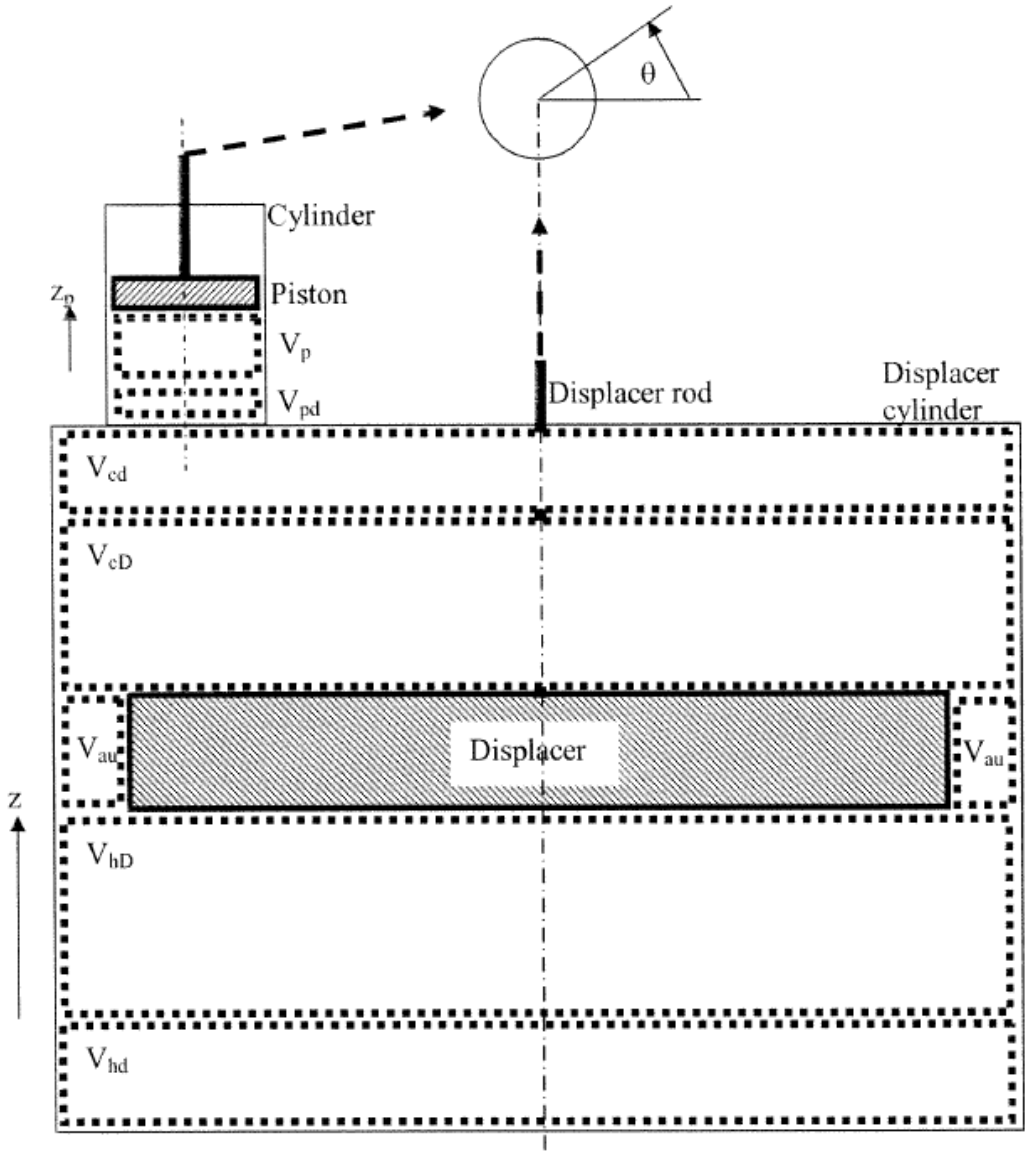

Fig. 4. Volumes in thermal-flow analysis.

shaft angle and speed as follows:

$$\frac{dp}{dz} = \frac{12\,\mu}{\pi\,D\,a^3}\left(ADc + \frac{\pi\,D\,a}{2}\right)\,Uz = -c0\sin(\theta)\,\omega \tag{9}$$

where $c0 = \frac{6\,\mu\,L}{\pi\,D\,a^3}\left(ADc + \frac{\pi\,D\,a}{2}\right)$ (10)

If the pressure gradient in the displacer annulus is approximated as:

$$\frac{dp}{dz} \sim \frac{pc-ph}{lD} \tag{11}$$

The pressure in the hot region of the engine can be related to pc, the pressure in the engine cold region, as :

$$ph \sim pc + c0\;lD\sin(\theta)\,\omega \tag{12}$$

The total amount of air in the engine is equal to the sum of air masses in different regions in the engine:

$$M = \rho c\,(Vp + Vpd + Vcd + VcD) + \rho h\,(VhD + Vhd) + \rho au\,Vau$$

(13)

The temperatures of air above and below the displacer are not uniform and depend strongly on the flow conditions. In the present thermodynamic analysis of the MM-7 engine, the following average temperatures are used for air above and below the displacer:

$$Tca = 0.5(Th + Tc) - 0.5(Th - Tc)(1 - Cc) \quad (14)$$

$$Tha = 0.5(Th + Tc) + 0.5(Th - Tc)(1 - Ch) \quad (15)$$

The temperature correction factors C_c and C_h, which are measurements of the departures of the average air temperatures from the engine cold- or hot- end temperatures T_c and T_h, should be close to zero at very low engine speeds. These factors are functions of Θ and ω, and shall increase as the engine speed increases. This is because there is insufficient time for effective heat transfer at high engine speeds.

Using the ideal-gas equation of state, the mass of air in the cold region of the engine is:

$$Mc = \frac{pc}{R\,Tca}\,(Vp + Vpd + Vcd + VcD) = pc\,[\,c1 + c2\cos(\theta) + c3\cos(\theta + \alpha)] \quad (16)$$

where

$$c1 = \frac{Vpd + Vcd + \frac{ADc\,L}{2} + \frac{Ap\,Lp}{2}}{R\,Tca} \quad (17),$$

$$c2 = \frac{-\frac{ADc\,L}{2}}{R\,Tca} \quad (18)$$

$$c3 = \frac{\frac{Ap\,Lp}{2}}{R\,Tca} \quad (19)$$

The mass of air in the hot region of the engine is:

$$Mh = \frac{ph}{R\,Tha}\,(VhD + Vhd) = pc\,[\,c4 + c5\cos(\theta)] + c6\sin(\theta)\,\omega + c7\cos(\theta)\sin(\theta)\omega \quad (20)$$

where

$$c4 = \frac{Vhd + \frac{ADc\,L}{2}}{R\,Tha} \quad (21),$$

$$c5 = \frac{\frac{ADc\,L}{2}}{R\,Tha} \quad (22)$$

$$c6 = c0\;lD\;\frac{Vhd + \frac{ADc\,L}{2}}{R\,Tha} \quad (23),$$

$$c7 = c0\;lD\;\frac{\frac{ADc\,L}{2}}{R\,Tha} \quad (24)$$

Assuming the air pressure and temperature in the displacer annulus are the averages of the pressures and temperatures in the regions above and below the displacer, the mass of air in the annulus can be computed from:

$$Mau = c8\,pc + c9\sin(\theta)\;\omega \quad (25)$$

where

$$c8 = 2\;lD\;\frac{ADc - A}{R\,(Tca + Tha)} \quad (26),$$

$$c9 = c0\;lD\;\frac{(ADc - A)\;lD}{R\,(Tca + Tha)} \quad (27)$$

Neglecting the small amount of air leaked through the gap between the displacer rod and its bushing and the gap between the piston and the power cylinder, the total amount of air in the engine remains constant during operation, and air pressure in the cold region of the engine can be expressed as a function of M, Θ and ω:

$$pc = \frac{M - [(c6 + c9)\sin(\theta)\omega + c7\cos(\theta)\sin(\theta)\,\omega]}{c1 + c4 + c8 + (c2 + c5)\cos(\theta) + c3\cos(\theta + \alpha)} \quad (28)$$

The moving-boundary work produce by the piston per cycle can be computed from the following integration:

$$Wb = \int_{\theta=0}^{2\pi} pc\, Ap\, dzp = -\frac{Lp}{2} Ap \int_{\theta=0}^{2\pi} pc \sin(\theta+\alpha)\, d\theta \quad (29)$$

The volumes of air in the gap of the long bushing of the displacer rod and in the annulus between the piston and the power cylinder are neglected in the above air volume calculations. These volumes are very small. Air flows through these 2 narrow flow channels are also neglected in the present thermodynamic analysis. The piston was replaced by a flexible membrane in an early version of this commercial LTD engine to eliminate air leakage in the power cylinder. Such a change probably caused too much resistance to the engine movement, and was later abandoned in favor of the air bearing design of the MM-7 engine.

Since the amount of air leaked to the surroundings when the engine pressure is higher than the surrounding air pressure is equal to the amount of air leaked into the engine when the engine pressure is lower than the ambient pressure, the surrounding work done on or by the leaked air canceled each other in a complete cycle. In a similar argument, the surrounding work when the piston moves upward is equal to (but opposite in sign) that when the piston moves downward. The net useful work output of the engine per cycle is therefore the moving-boundary work of the air underneath the piston minus the work required to overcome the viscous frictions on the lateral surfaces of the piston, the displacer, and the displacer rod, and the work required to overcome the pressure difference across the displacer.

Using the analytical solutions for steady, fully developed, incompressible laminar flow between 2 parallel plates or in an annulus, the shear stresses on the lateral surfaces of the displacer, the piston, and the displacer rod are:

$$\tau = \mu \frac{Uz}{a} + \frac{a}{2}\frac{dp}{dz} \quad (30),$$

$$\tau p = \frac{\mu\, Uzp}{rp \ln\left(\frac{rp}{rp+ap}\right)} \quad (31)$$

$$\tau DR = \frac{\mu\, Uz}{rDR \ln\left(\frac{rDR}{rDR+aDR}\right)} \quad (32)$$

The shear stresses due to pressure differences are neglected in Eqs. (31) and (32) since these 2 flow channels are very long and narrow. The flows can be approximated by the Couette flow.

The corresponding shear forces and work required to overcome the viscous drags per cycle are:

$$\tau = \mu \frac{Uz}{a} + \frac{a}{2}\frac{dp}{dz} \quad (30),$$

$$Fs = \pi\, D\, lD\, \tau \quad (33)$$

$$Fsp = \pi\, Dp\, lp\, \tau p \quad (34),$$

$$FsDR = 2\pi\, rDR\, lDR\, \tau DR \quad (35)$$

$$Ws = \int_{\theta=0}^{2\pi} Fs\, dz = -\frac{L}{2}\int_{\theta=0}^{2\pi} Fs \sin(\theta)\, d\theta \quad (36)$$

$$Wsp = \int_{\theta=0}^{2\pi} Fsp\, dzp = -\frac{Lp}{2}\int_{\theta=0}^{2\pi} Fsp \sin(\theta+\alpha)\, d\theta \quad (37)$$

$$WsDR = \int_{\theta=0}^{2\pi} FsDR\, dz = -\frac{L}{2}\int_{\theta=0}^{2\pi} FsDR \sin(\theta)\, d\theta \quad (38)$$

The work required to overcome the pressure difference across the displacer per cycle can be calculated from:

$$Wpd = \int_{\theta=0}^{2\pi} (pc-ph)\, A\, dz = -\frac{L}{2}\int_{\theta=0}^{2\pi} (pc-ph)\, A \sin(\theta)\, d\theta \quad (39)$$

The net work per cycle multiplied by the engine speed (in RPS) gives the engine power output (in Watts).

Air pressure in the cold region of the engine is expected to be pretty uniform at any instance for low engine speeds. As a result, the boundary work

produced by the piston can be determined by measuring the time variation of air pressure in the cold region of the engine and the piston displacement.

The mechanical power outputs of the MM-7 engine had been measured in Aragon - Gonzalez et al.'s paper [8] and in Alveno et al.'s experiments [7] for different engine speeds and temperature differentials. A dynamometer was employed in Aragon - Gonzalez et al.'s experiments to measure the engine mechanical power. Alveno et al. measured the rate of change in height of a mass lifted by the engine to determine the engine power output. The engine powers measured in these 2 publications are in good agreement, especially at low engine speeds. For instance, at ω around 2π rad/s (=1 RPS) and ΔT = 20℃, the measured mechanical power output was about 2mW in Aragon - Gonzalezetal.'s paper, and about 1.7mW in Alvenoetal.'s report.

3. Results and discussions

The phase difference between the piston and displacer movements has a significant impact on the engine power output. In theory, the cyclic power output is positive (i.e., a power cycle) when heat is added to the cycle during compression and removed from the cycle during expansion of the working fluid. As shown in the boundary work plot in Fig. 5, the work output of the piston (wb) is positive for α = - π to 0, and negative for α = 0 to π. The boundary work of the piston reached its maximum value at α = - π/2. The other forms of work (w_s, w_{sp}, w_{sDR}, and w_{pd}) are almost independent of α and much smaller than wb. Therefore, the net work output of the engine is maximum when α is around - π/2. The results and discussions in the remainder of this section are for this optimal phase angle.

The pressure in the engine is at the ambient pressure before the engine starts running. The crank angle at which p_c is equal to the ambient pressure (p_o) was found to affect w_b only slightly, with w_b at its maximum value for Θ_o (the crank angle at which p_c = p_o) = π/2.

The computed air pressure variation in the cold region of the engine and the difference between p_c and p_h are presented in Fig. 6 for ω = 1 to 10 RPS,

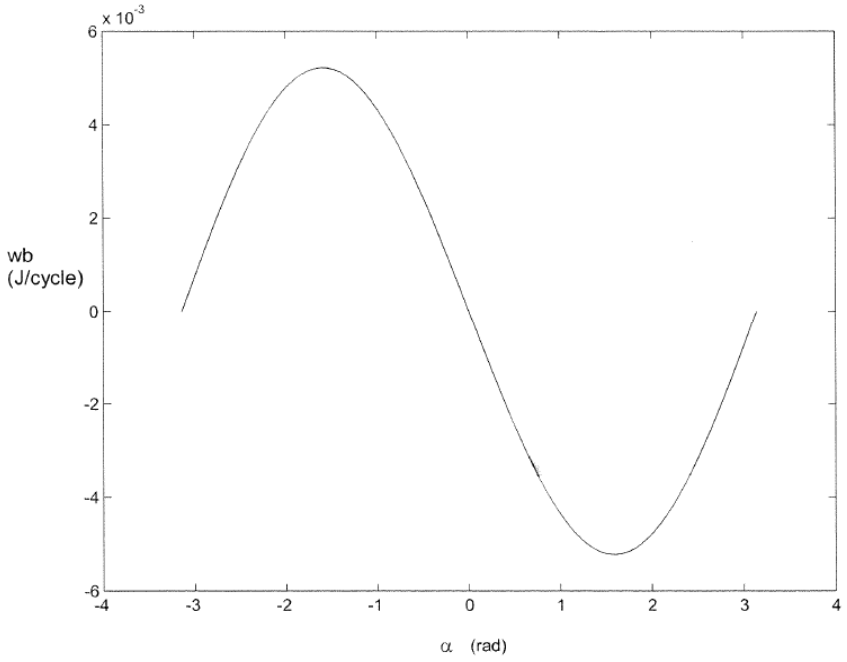

Fig. 5. Moving- boundary work produced by the piston for different phase differences. (ΔT=20℃, ω =1 RPS, C_c=C_h=0).

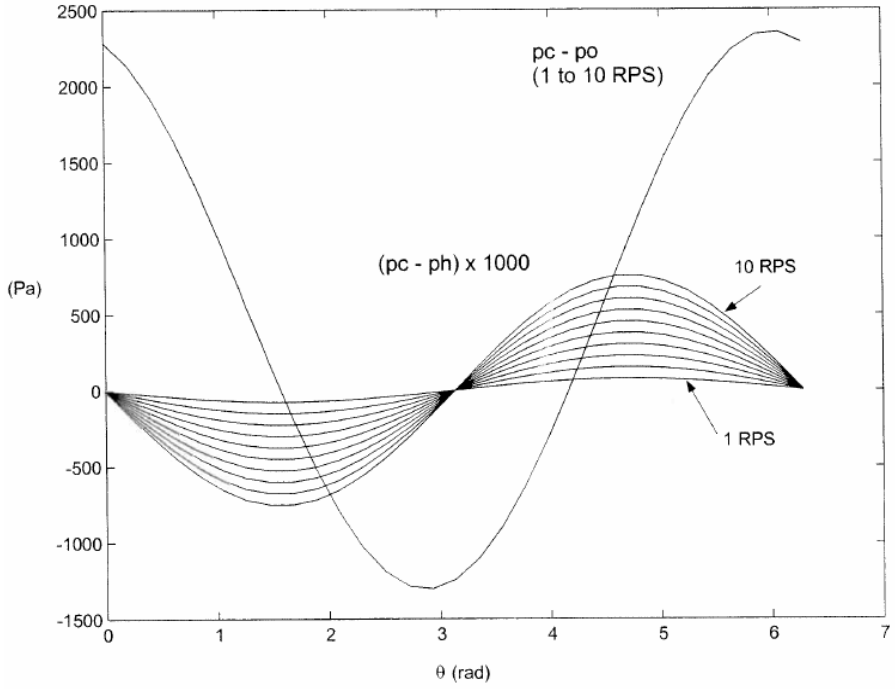

Fig. 6. Pressure and pressure difference in the displacer cylinder for different engine speeds. (ΔT=20℃, ω =1 to 10 RPS, C_c=C_h=0).

ΔT = 20℃, and no temperature corrections (C_c=C_h=0). The pressure difference across the displacer increases with engine speed, but p_c is almost independent of ω for engine speeds below 10 RPS. According to the ideal-gas law, the air pressure increases with temperature but decreases with volume for a fixed mass. It is interesting to note that the maximum pc does not occur at Θ = 0 at which the volume of high-temperature air (V_{hD} + V_{hd}) is maximum, nor at Θ = - π/2 at which the total volume of air (=sum of all the volumes highlighted by the dotted lines in Fig. 4) in the engine is minimum. The maximum p_c occurs at an angle between Θ = - π/2 and 0 at which most of the displacer cylinder is filled with high-temperature air while the total volume of air in the engine is slightly greater than its minimum value.

The calculated shear stresses on the lateral surfaces of the piston, the displacer, and the displacer rod are presented in Fig. 7 for ω = 1 RPS, ΔT = 20℃, and C_c=C_h=0. Because of the sinusoidal movements of the piston and the displacer, and the 90 degree phase difference between the 2 movements, the shear stresses on the piston and the displacer are sinusoidal functions of Θ and are 90 degrees out of phase. Although τ_p is the highest and τ the lowest shear stress in this plot, the displacer has the largest lateral surface area. Therefore, the work required to overcome the viscous drag on the displacer is greater than the viscous work on the piston.

Shown in Figs. 8(a) to 8(c) are the engine net power outputs for different engine speeds and temperature differentials. Different forms of work per unit time are presented in Fig. 9 for ΔT = 20℃ and C_c=C_h=0. The temperature correction factors C_c and C_h were assumed to be independent of engine speed in these calculations. As a result, the boundary work produced by the piston per unit time is almost a linear function of ω. It should be pointed out that, as the engine speed increases, there will be less time for effective heat transfer between the working fluid and the hot or cold end of the engine, and the temperature correction factors should increase. A comparison of the 3 plots in Fig. 8 indicates that the

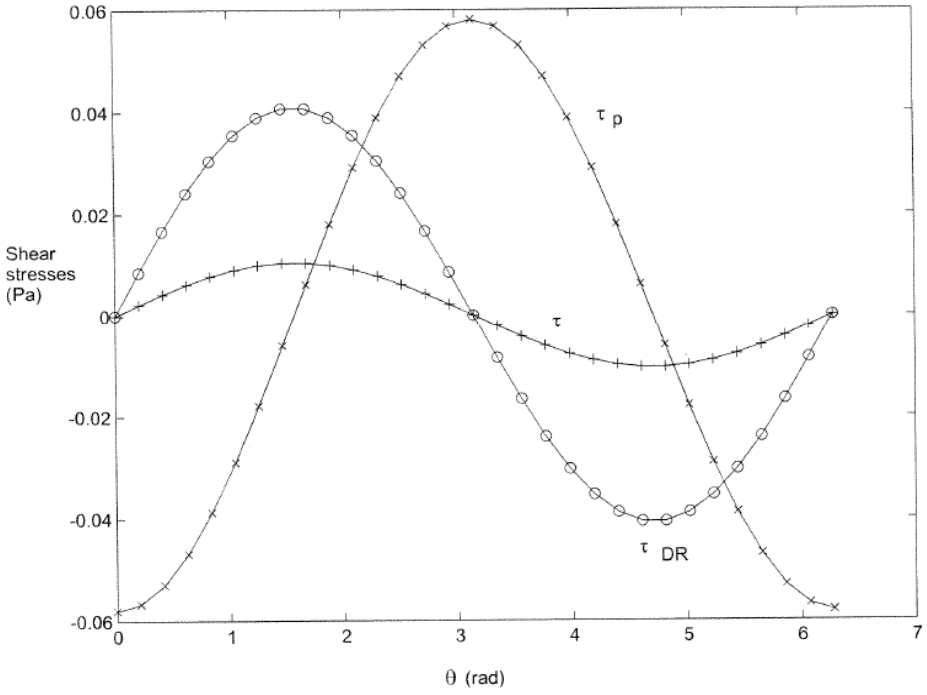

Fig. 7. Shear stresses on the lateral surfaces of the piston and the displacer. (ΔT=20℃, ω =1 RPS, C_c=C_h=0).

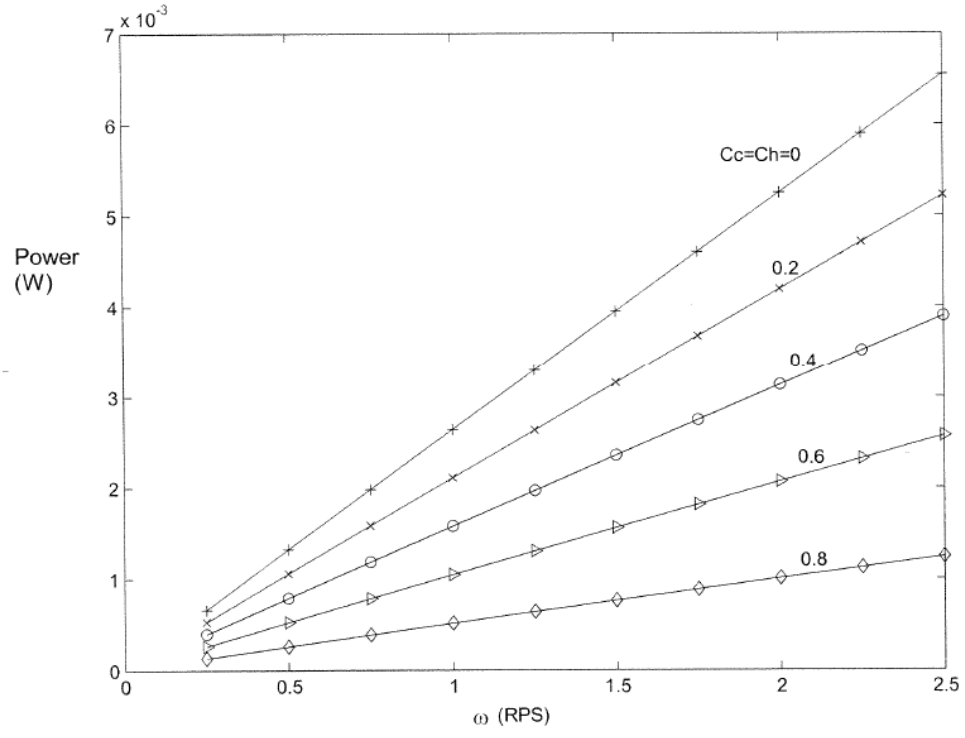

(a)

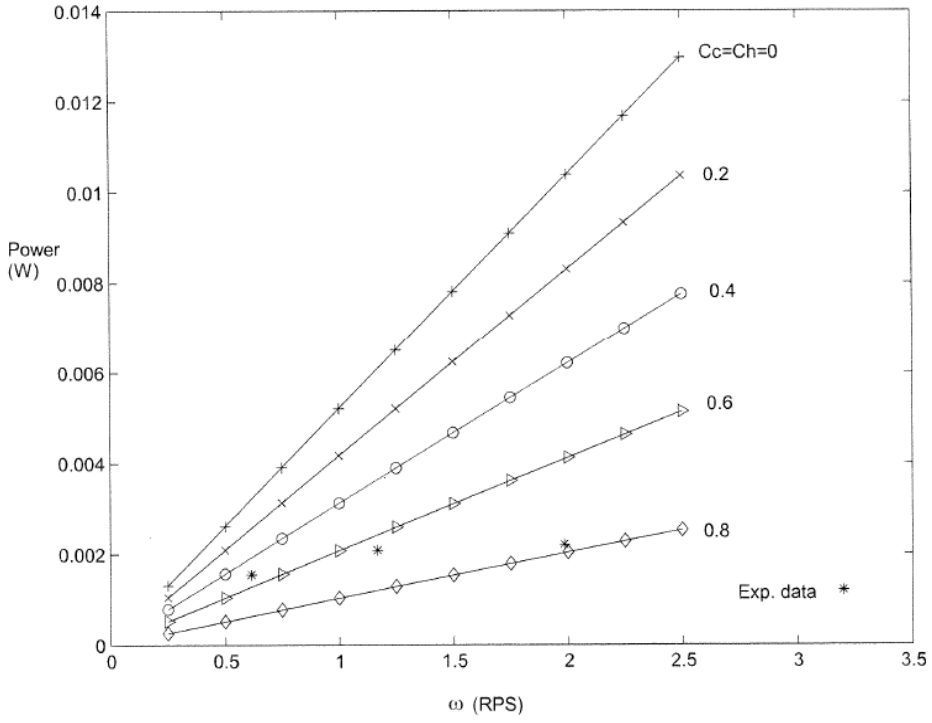

(b)

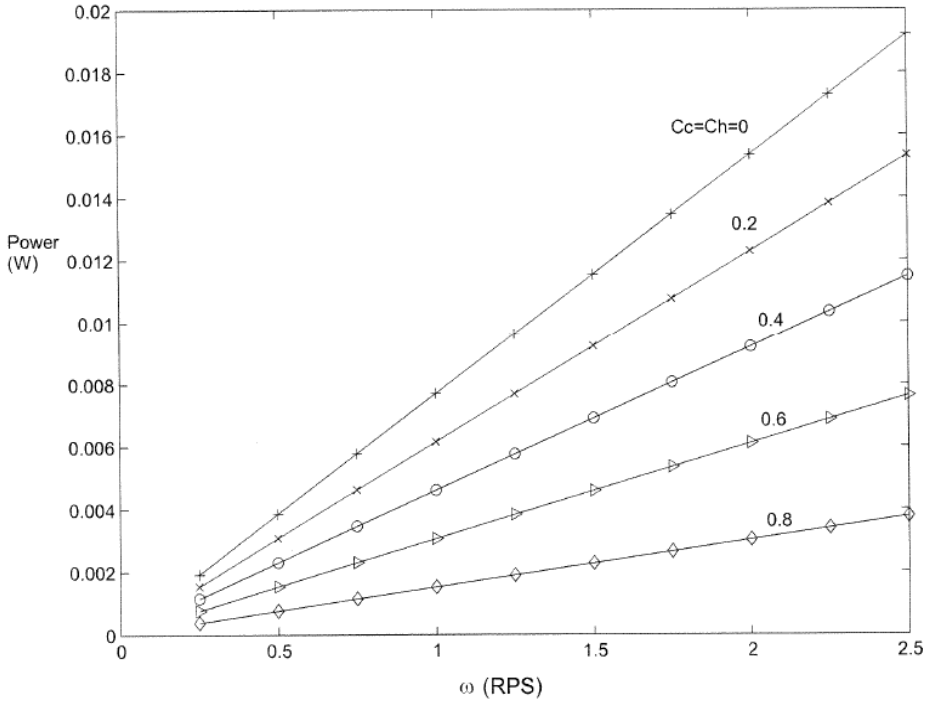

(c)

Fig. 8. Calculated engine power outputs for different temperature differentials. (a) ⊿T=10℃, (b) ⊿T=20℃, (c) ⊿T=30℃.

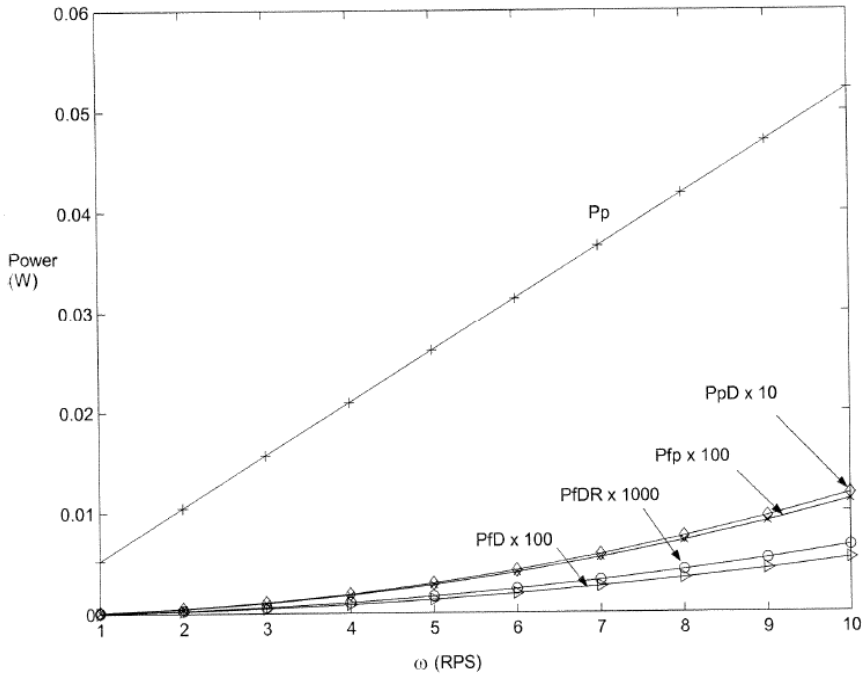

Fig. 9. Different forms of work produced or consumed by the engine per unit time for ⊿T=20℃, ω = 1 to 10 RPS, and Cc=Ch=0. (Pp = boundary work produced by the piston per unit time; Pfp, PfDR, and PfD = power required to overcome the viscous drags on the piston, the displacer rod, and the displacer; PpD = power required to overcome the pressure difference across the displacer).

relationship between engine power output and temperature differential at a given engine speed is also almost linear.

As can be seen in Fig. 9, for ω < 10 RPS and ΔT in the neighborhood of 20℃, the work required to overcome the viscous frictions on the piston and the displacer is much smaller than the boundary work produced by the piston.

Even at ω = 10 RPS, the work required to overcome the pressure difference across the displacer is one-to-two orders of magnitude smaller than the work produced by the piston. Thus, the degradation from the ideal engine performance is primarily due to the ineffective heat transfer during heat addition and rejection.

Comparing the calculated engine power outputs with those measured in Aragon-Gonzalez et al.'s experimental study of the MM-7 engine [8] for ΔT = 20℃ (data"*"in Fig. 8(b)), the temperature correction factors are about 0.5 for ω < 1 RPS, but increase to more than 0.8 at ω > 3 RPS, meaning the change in the working fluid temperature when heat was transferred to or from the cold or hot end of the engine was less than 20% of the maximum possible temperature change for ω > 3 RPS. This result clearly indicates that heat transfer from the engine hot or cold end to the air in the MM- 7 engine is very ineffective at high engine speeds. Fins and/or other heat transfer-enhancing devices should be installed inside the displacer cylinder to improve heat transfer during heat addition and rejection.

4. Conclusions

The thermodynamics and fluid flow of the American Stirling Company MM-7 engine were studied theoretically. The optimal phase angle between the

piston and displacer movements that maximizes the engine power output is about 90 degrees. The maximum pressure in the engine occurs at a crank angle between the angle corresponding to minimum air volume in the engine and the angle at which the volume occupied by the high-temperature air reaches it maximum value. Of the different forms of work produced or consumed by the piston and the displacer, the moving-boundary work of the piston increases nearly linearly while the other forms of work increase more rapidly as the engine speed increases. Compared with the boundary work produced by the piston movement, the work required to overcome the viscous drags on the piston, the displacer, and the displacer rod was found to be very small for engine speeds below 10 RPS. The boundary work of the displacer is also one-to-two orders of magnitude smaller than that of the piston for temperature differentials around 20℃ and engine speeds below 10 RPS. A comparison of the calculated engine power outputs with experimental data reveals very ineffective heat transfer between the working fluid and the engine hot and cold ends for engine speeds above 1 RPS. Fins or other heat-transfer devices are recommended to enhance heat transfer inside the displacer cylinder for higher engine power output and thermal efficiency.

Acknowledgments

The authors would like to acknowledge the support from the National Research Foundation of Korea through the Ministry of Science, ICT & Future Planning
(Grant Number: 2014R1A2A1A01006421).

References

1. Cengel, Y. A., Boles. M. A., 2015, Thermodynamics: An Engineering Approach, 8th Edition, McGraw Hill., New York, USA, pp. 275-313.
2. Shirani, M., Kadkhodaei. M., 2016, One-dimensional constitutive model with transformation surfaces for phase transition in shape memory alloys considering the effect of loading history, International Journal of Solids and Structures, Vol. 81, pp. 117-129.
3. Chen, K., Gwilliam. S. B., 1996, An analysis of the heat transfer rate and efficiency of TE (Thermoelectric) cooling systems, International Journal of Energy Research, Vol. 20, No. 5, pp. 399-417.
4. Riba, J. R., et al., 2016, Rare-earth-free propulsion motors for electric vehicles: A technology review, Renewable and Sustainable Energy Reviews, Vol. 57, pp. 367-379.
5. Rizzo, J. G., 1995, The Stirling engine manual, Camden miniature steam service.
6. Senft, J. R., 1993, Ringbom Stirling Engines, Oxford University Press, New York, USA.
7. Alveno, D., et al., 2105, Electricity harvesting from low temperature waste heat, ME EN 4010 Final Design Report (faculty advisors: K. Chen and S. Roundy), Mechanical Engineering Department, University of Utah, USA.
8. Aragon-Gonzalez, G., et al., 2013, Developing and testing low cost LTD Stirling engines, THERMODYNAMICS, Revista Mexicana de Fisica, Vol. 50, No. 1, pp. 199-203.